

Conformational analysis of α,β -poly(*N*-hydroxyethyl)-*DL*-aspartamide (PHEA) and α,β -polyasparthydrazide (PAHy) polymers in aqueous solution

Tommasina Coviello^{a,*†}, Yoshiaki Yuguchi^a, Kanji Kajiwara^a, Gaetano Giammona^b, Gennara Cavallaro^b, Franco Alhaique^c and Antonio Palleschi^d

^aFaculty of Engineering and Design, Kyoto Institute of Technology, Kyoto, Japan

^bDepartment of Chemistry and Pharmaceutical Technologies, University of Palermo, Via Archirafi 32, 90123 Palermo, Italy

^cDepartment of Studies of Chemistry and Technology of Biologically Active Compounds, University 'La Sapienza', P.le A. Moro 5, 00185 Rome, Italy

^dDepartment of Chemistry, University 'La Sapienza', P.le A. Moro 5, 00185 Rome, Italy

(Received 4 September 1997; revised 15 December 1997; accepted 16 December 1997)

α,β -Poly(*N*-hydroxyethyl)-*DL*-aspartamide (PHEA) and α,β -polyasparthydrazide (PAHy) are synthetic polymers previously studied for biomedical applications. We report here the results of a small-angle X-ray scattering analysis carried out on these two macromolecules in aqueous solution. The data obtained indicate that the two polymers assume remarkably different conformations in aqueous solution, although the backbone is supposed to be the same for the two chains. PHEA can be represented by a random coil conformation, whereas PAHy can be described in terms of an elliptical cylinder characterized by an almost planar structural arrangement with the backbone refolded on itself in a fashion somewhat similar to the β layer of globular proteins. This more rigid conformation of PAHy is related both to the network of hydrogen bonds capable of stabilizing the overall structure and to the lower molecular weight with respect to PHEA. Conformational and energetic analyses of PAHy are also discussed. © 1998 Elsevier Science Ltd. All rights reserved.

(Keywords: SAXS; conformational analysis; polymer structure)

Introduction

α,β -Poly(*N*-hydroxyethyl)-*DL*-aspartamide (PHEA) and α,β -polyasparthydrazide (PAHy) are two synthetic macromolecules (Figure 1) with a protein-like structure that show interesting properties related to many potential applications in the field of biomedical sciences^{1–6}. Furthermore, in the last few years we have undertaken a systematic study on the physico-chemical properties of these two polymers^{7–12} in order to provide useful information to rationalize the functions *in vivo* of macromolecules of biological interest¹³.

Calorimetric investigations of the interaction between PHEA and micelles of anionic, cationic and non-ionic surfactants have suggested that this macromolecule shows a positive charge density in aqueous media⁷. In the case of PHEA–sodium dodecyl sulfate micelles, the presence of a simple electrolyte (NaCl) allows a distinction between the electrostatic and the hydrophobic contribution to micelles interaction⁸. Viscometric investigation of PHEA aqueous solutions indicated that it acts as a strongly hydrated random coil⁹. Furthermore, the structural and dynamic dielectric properties of aqueous solutions of these polymeric carriers evidenced that PHEA and PAHy macromolecules interact with water molecules, essentially through hydrogen binding¹². In this study we investigated the structure of PHEA and PAHy in aqueous solutions by mean of small-angle X-ray scattering (SAXS). The technique is suitable for observing particles of dimensions 10–500 Å and, therefore, can give information on the structure of most

macromolecular systems like biological or synthetic polymers. Conformational and energetic analyses of PAHy are also discussed.

Experimental

Materials and methods

Sample preparation. All the reagents used were of analytical grade, otherwise stated.

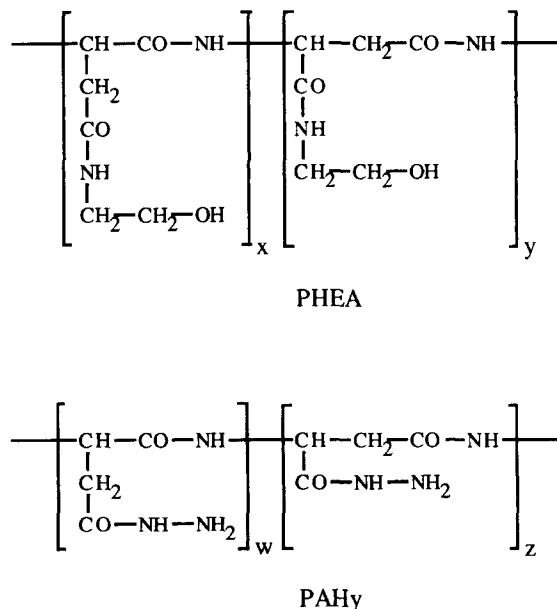


Figure 1 Repeating unit of PHEA and PAHy

* To whom correspondence should be addressed

† Permanent address: Department of Studies of Chemistry and Technology of Biologically Active Compounds, Rome, Italy

D,L-Aspartic acid, ethanolamine and hydrazine monohydrate were obtained from Fluka (Switzerland); *N,N*-dimethylformamide (DMF) (Hoechst) was dried with P_2O_5 and then distilled under reduced pressure before use. PHEA ($[\eta]=26 \text{ ml g}^{-1}$ in water) was prepared by reaction

of polysuccinimide (PSI) with ethanolamine in DMF solution according to a procedure reported elsewhere¹⁴. PAHy ($[\eta]=12 \text{ ml g}^{-1}$ in water) was prepared by reaction of PSI with hydrazine in DMF solution according to a previously reported procedure^{2,15}.

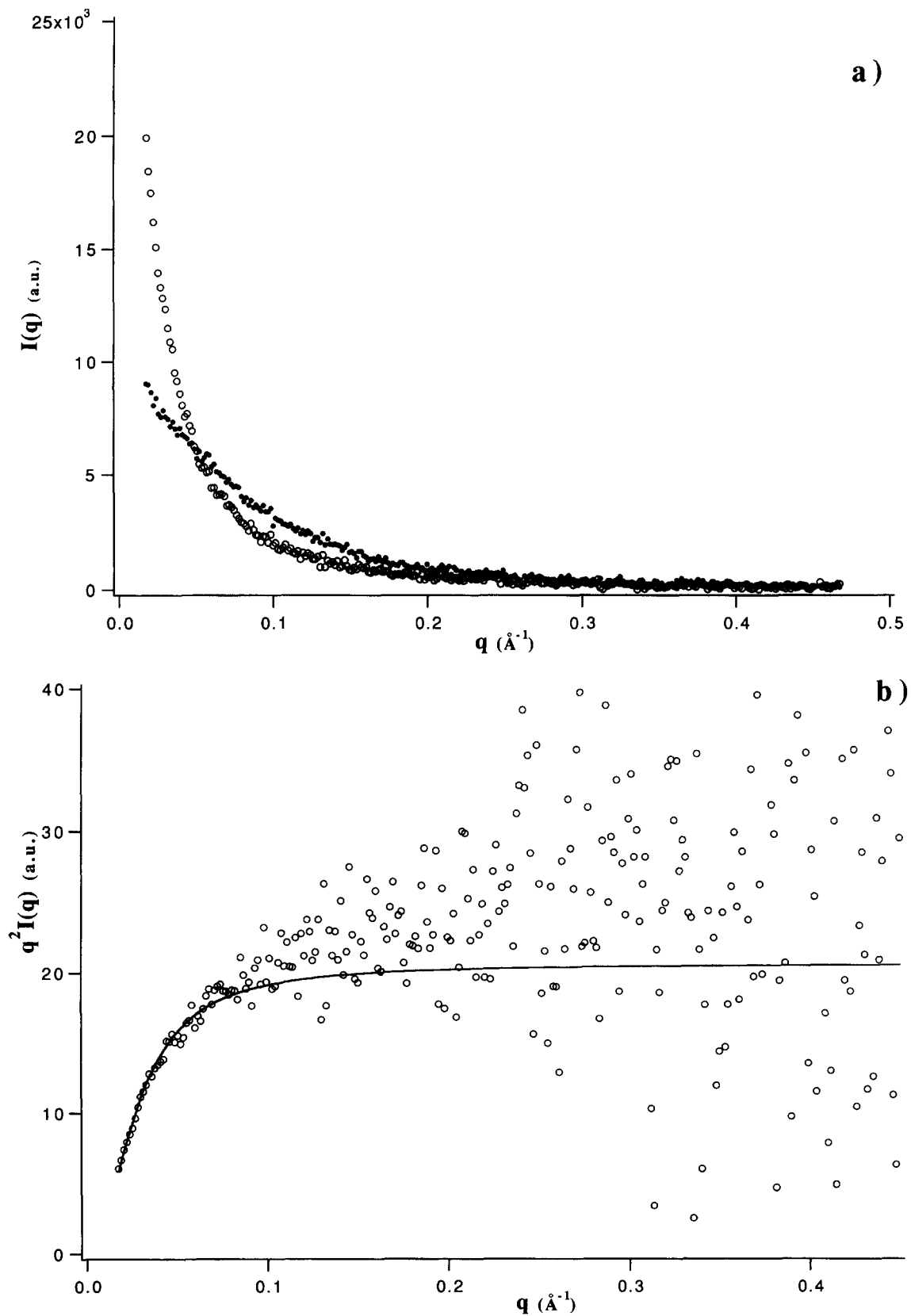


Figure 2 (a) SAXS from PHEA (O) and PAHy (●) aqueous solutions in 0.1 M NaCl at 20°C; $c_p = 0.9\%$ (w/v). (b) Kratky plot from PHEA (O) and the Lorentzian fitting (—) assuming $\xi = 35.3 \text{ \AA}$. (c) Kratky plot from PAHy (●) and the elliptic cylinder model (—) assuming the semiaxes values equal to 2.4, 12.9 and 33.0 Å

PAHy and PHEA weight-average molecular weights M_w were measured by light scattering (LS) on a Dawn DSP-F Laser Spectra Physics spectrometer.

The solutions for SAXS measurements were prepared by dissolving the lyophilized polymers in water and then adding the appropriate amount of NaCl to reach the final polymer concentration $c_p = 0.9\%$ (w/v) in 0.1 M NaCl. The concentrations used were well below the overlap concentration c^* and, therefore, aggregation could be neglected for the data analysis.

The conformational studies were carried out using in-house software.

SAXS. The SAXS measurements were performed at BL-10C of the Photon Factory, Tsukuba, Japan¹⁶. Incident X-rays from synchrotron radiation were monochromatized to $\lambda = 1.49 \text{ \AA}$ with a double-crystal monochromator, and focused with a focusing mirror. The scattered X-rays were detected by a one-dimensional position-sensitive proportional counter (PSPC) positioned approximately 1 m from the sample holder. A flat sample cell of 0.2 cm path-length (made of glass) with $1.2 \text{ mm} \times 0.3 \text{ mm}$ quartz windows was used. The cell was thermostatically controlled by circulating water at a constant temperature through the cell holder. The solution was injected into the thermostatic cell at a prefixed temperature (20°C) and maintained at that temperature for several minutes prior to the SAXS measurement.

The SAXS intensities were accumulated for 600 s in order to assure a sufficient statistical accuracy without degrading the samples by X-radiation. The scattered intensities were corrected, with respect to the variation of the incident X-ray flux, by monitoring an ion chamber installed in front of the cell holder and the X-ray absorption of the solution by measuring the incident and transmitted

X-ray intensities. The excess scattering intensities were evaluated by subtracting the scattering intensities of the solvent from those of the PHEA and PAHy solutions.

Results and discussion

SAXS. Figure 2a–c shows the SAXS results from the PHEA and PAHy samples in 0.1 M NaCl aqueous solution in terms of the normal plots (a) and the Kratky plots¹⁷ ($q^2 I(q)$ versus q) (b and c). Here q is the magnitude of the scattering vector given by $(4\pi/\lambda) \sin \theta$ with θ and λ being a half of the scattering angle and the wavelength of incident X-rays respectively.

Both PHEA and PAHy are specified as the block copolymer composed of the backbone units of $-\text{CH}-\text{CO}-\text{NH}-$ and $-\text{CH}-\text{CH}_2-\text{CO}-\text{NH}-$ (see Figure 1). According to the reaction scheme², the degree of polymerization for each unit (X and Y for PHEA, and W and Z for PAHy) can be adjusted independently, but no experimental data allow identification of the actual sequence of the monomers in the macromolecules. Nevertheless, it can reasonably be assumed that the primary structure of the main chain of both PHEA and PAHy should be the same in the present case. The two polymers exhibit different scattering characteristics that can be related to different configurations; so, we may expect that one polymer is flexible and the other is stiff, despite the same backbone structure.

The observed differences can be shown even better by the cross-sectional Guinier plot¹⁸ shown in Figure 3 for both samples.

The cross-sectional Guinier plot can be properly applied only in the case of elongated particles for which the total scattering intensity $I(q)$ can be split into two factors

$$I(q) \approx I_c(q) \times 1/q \quad (1)$$

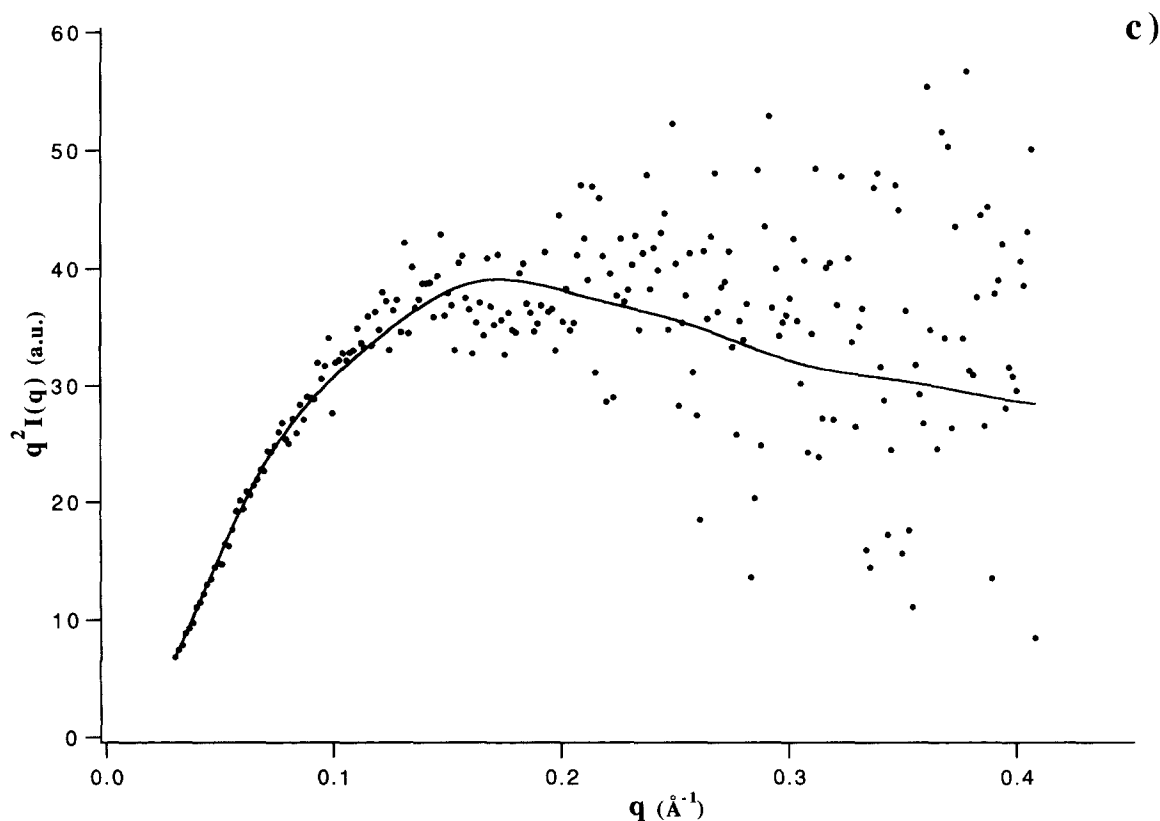


Figure 2 Continued

The first factor $I_c(q)$ is derived from the dimensions and the shape of the cross-section and the Guinier-like approximation leads to the expression

$$I_c(q) \approx \exp(-q^2 R_{gc}^2/2) \quad (2)$$

where R_{gc} denotes the cross-sectional radius of gyration. The second term $1/q$ is characteristic of a rod-like molecule¹⁹ and indicates that the cross-sectional Guinier plot ($\ln[qI(q)]$ versus q^2) yields a straight line specified by a slope $R_{gc}^2/2$.

Indeed, for PAHy, the initial part of the intensity can be nicely fitted by a straight line (indicating the presence of a stiff structure), whereas in the case of PHEA a curvature is observed in the whole range of q explored (thus, here, the presence of a stiff structure can be excluded).

The Kratky plots (\circ, \bullet in Figure 2b and c) confirm and broaden the information acquired by means of the Guinier cross-sectional plots revealing the structural difference between the two polymers. As evidenced by the trend of

the fitting curves, PHEA has a rather flexible configuration (presence of a plateau), whereas PAHy has a compact structure (a maximum appears at intermediate q values).

The radii of gyration R_G were evaluated as 57 Å for PHEA and 20 Å for PAHy from the initial slope of the respective Zimm plots²⁰ which read as

$$I(q)^{-1} \approx \frac{1}{3} R_G^2 \quad (3)$$

The values of the radius of gyration also indicate the compactness of PAHy even when the difference of the molecular weight (see Table 1) is taken into account.

In order to analyse the structure of PHEA and PAHy in more detail, the SAXS profiles were fitted to the scattering profiles calculated from two models. Since PHEA is thought to be flexible²¹, the Debye²² function and the Ornstein-Zernike²³ approach were applied. A better fitting was obtained with the Ornstein-Zernike function, where the distance density correlation $\gamma(r)$ of the PHEA chain is approximately represented by

$$\gamma(r) \approx (\xi/r) \exp(-r/\xi) \quad (4)$$

which yields the Lorentzian scattering

$$I(q) \approx 1/(1 + \xi^2 q^2) \quad (5)$$

where r denotes a distance between two points on the chain. Equation (4) is a good representation of a Gaussian chain in the intermediate r range, and the correlation length ξ is equivalent to the radius of gyration R_G in the case of an isolated chain (a dilute solution), as seen from equations (3) and (4) where

$$R_G = 3^{1/2} \xi \quad (6)$$

The curve reported in Figure 2b shows the results of the fitting by means of equation (4) with $\xi = 35.3$ Å (equivalent

Table 1 Molecular weight M_w , intrinsic viscosity $[\eta]$, radius of gyration R_G , correlation length ξ and half-axis lengths a, b, c of the ellipsoid for PHEA and PAHy samples

	PHEA	PAHy
M_w^a	52×10^3	23×10^3
$[\eta]^b$ (ml g ⁻¹)	26	12
R_G (Å)	61.1	20.1
	56.6 ^c	21.7 ^c
ξ (Å)	35.3	
a (Å)		12.9
b (Å)		2.4
c (Å)		33.0

^a From LS data

^b In water, 25°C

^c From Zimm plot

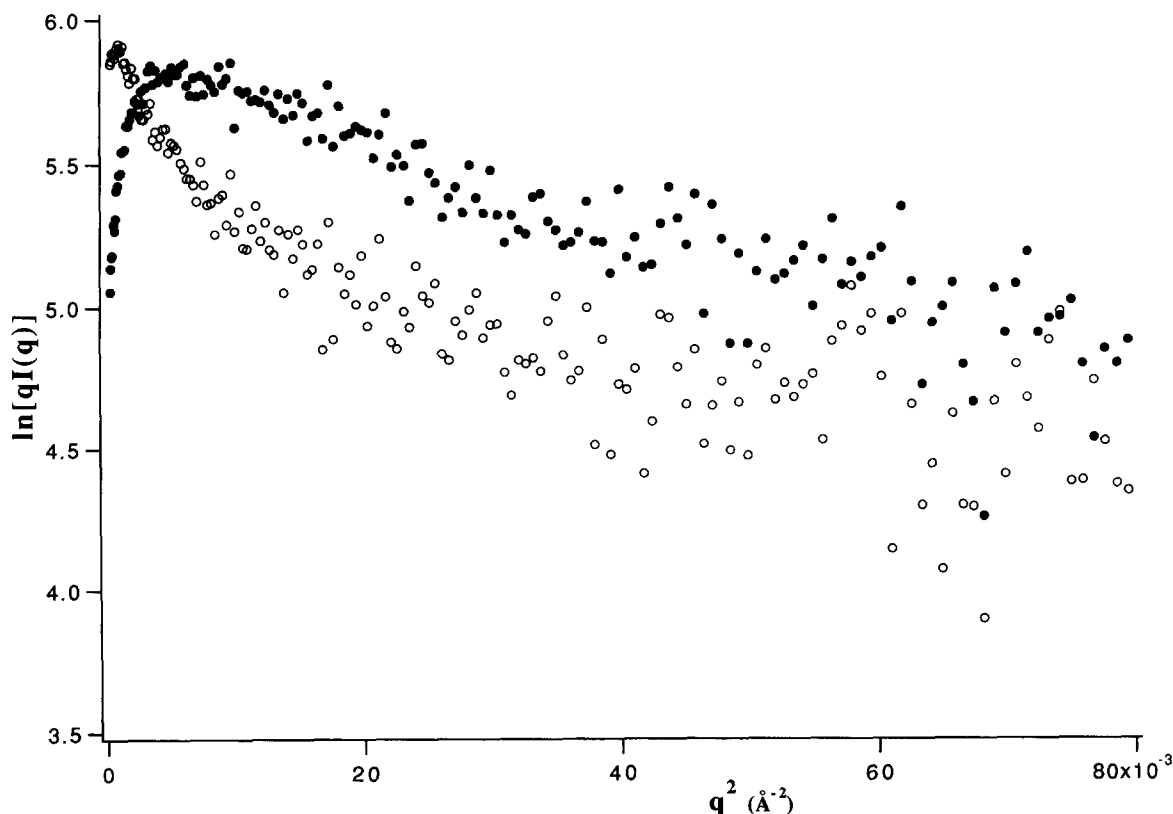


Figure 3 Cross-sectional Guinier plots for SAXS from PHEA (\circ) and PAHy (\bullet) aqueous solution in 0.1 M NaCl at 20°C; $c_p = 0.9\%$ (w/v)

to $R_G = 61 \text{ \AA}$). On the other hand, a triaxial body of a homogeneous density is assumed to represent the shape of the compact PAHy, as shown by the curve in Figure 2c. The SAXS profile of PAHy was fitted to the scattering profile calculated from an ellipsoid, where a thin ellipsoid of $12.9(a) \times 2.4(b) \times 33.0(c) \text{ \AA}^3$ was found to yield the best-fit scattering profile.

The parameters evaluated from the fitting are summarized in Table 1. Two independent evaluations (by Zimm plots and the model fittings) yielded consistent values of the radius of gyration, confirming that the assumed models were appropriate. The molecular weights by LS are estimated as 52 000 for PHEA and 23 000 for PAHy. The extrapolated values of $I(q)$ for $q \rightarrow 0$ are proportional to the molecular weight, so that the intercepts at $q = 0$ of the SAXS profiles (Figure 2a) correspond to the relative molecular weights of two polymers. Here the ratio of the molecular weight of PHEA to that of PAHy was estimated as *ca.* 2.6 by assuming

the same density for the two polymers. The value is consistent with the molecular weight obtained from the LS data reported in Table 1.

Conformational and energetic analysis. Conformational energy calculations were carried out using the set of parameters previously reported²⁴⁻²⁸.

The total potential energy was evaluated in terms of non-bonding, electrostatic, and hydrogen bond interactions, with a refinement process that minimizes the conformational energy in the multidimensional space of all torsional angles. Standard bond angles and bond lengths were used for both the backbone and side-chains^{29,30,31}. Non-bonded interatomic interactions were evaluated using a 6-12 LJ potential function²⁴⁻²⁸, and Coulombic interactions were assessed by assigning partial atomic charges for each atom in the macromolecule and a distance-dependent dielectric constant²⁴⁻²⁶.

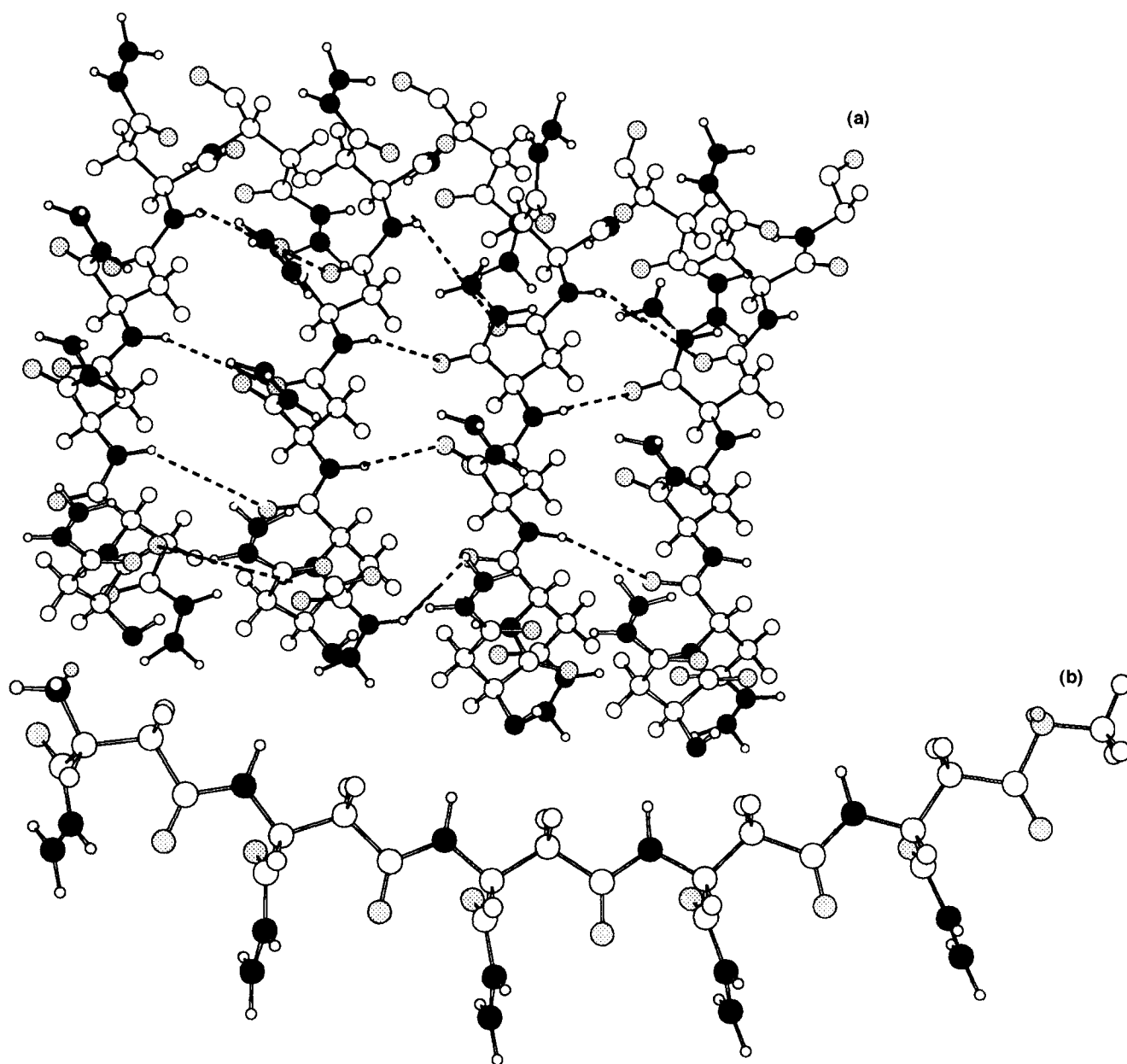


Figure 4 (a) Representation of a possible assembly of a portion of the PHAy macromolecule characterized by a regular sequence of short and long units. Dotted lines represent the hydrogen bonds. (b) Representation of a sequence of consecutive short side-chain units leading to a curvature of the backbone axis ($\circ = \text{C}$; $\odot = \text{O}$, $\circ = \text{H}$, $\bullet = \text{N}$)

Among the various results obtained from the SAXS measurements, particular attention should be focused on the reduced dimensions of the thin ellipsoid calculated for PAHy. In fact, a thickness of about 5 Å can be obtained only by a planar structural arrangement with the backbone refolded on itself in a fashion somewhat similar to the β layer of globular proteins. In other words, the SAXS data allowed us to reject the helical structures characterized by a network of intrachain hydrogen bonds (i.e. α -helix), which yields a thickness of more than 5 Å. The main difference between the β sheet of the proteins and that of PAHy is that the NH and CO groups cannot be in phase because of the random insertion of methylenic groups in the backbone. Accordingly, the intramolecular hydrogen bonds between the chains are not regularly distributed. However, the ordered structure could be stabilized by hydrogen bonds between the NH of the side chains and the free CO groups of the backbone. In *Figure 4a* a sketch of a possible assembly of a portion of the macromolecule is shown. This structure, characterized by a regular sequence of short and long units, is stabilized by a network of hydrogen bonds. Since a previous n.m.r. study, carried out on PHEA, indicates that short and long side-chains are present in a 1:1 ratio³², the same distribution of the short and long side-chains is expected in the case of PAHy. Furthermore, the structure with an alternate short-long side-chain regular sequence, can be supported by a theoretical calculation that allows us to formulate a hypothesis concerning the mechanism of the polymer formation. In fact, as reported in *Figure 4b*, a sequence of consecutive short side-chains leads to a curvature of the backbone axis and, consequently, is not compatible with the formation of the required parallel chains.

Conclusions

From the results obtained it is interesting to point out that PHEA and PAHy are supposed to have the same backbone but reveal a remarkable conformational difference in aqueous solution. Such a difference can be attributed to the variation of the side-chains as well as to a difference in polarity, although due account should be taken of the higher molecular weight of PHEA. The longer and more hydrophilic side-chains of PHEA play a fundamental role in the high solubility shown by this polymer in water and in several other polar solvents (e.g. DMF). The flexibility of the backbone due to the presence of the methylenic groups and the interactions of the side-chains with water molecules do not prevent a random coil conformation, as shown for PHEA by SAXS data. On the other hand, in the case of PAHy, the proposed more rigid conformation, described by an elliptical cylinder, is to be related both to the network of hydrogen bonds capable of stabilizing the overall structure and to the quite low molecular weight. In fact, the suggested thin ellipsoid model could not be proposed if PAHy had a higher molecular weight because a collapsing effect would occur for the β -sheet structure.

Acknowledgements

One of us (T.C.) thanks the C.N.R. and the J.S.P.S. for a fellowship. The work was performed under the approval of the Photon Factory Advisory Committee (Proposal No. 91-217).

References

- Giammona, G., Carlisi, B., Pitarresi, G. and Fontana, G., *J. Bioact. Comp. Polym.*, 1991, **6**, 129.
- Giammona, G., Carlisi, B., Cavallaro, G., Pitarresi, G. and Spampinato, S., *J. Controlled Release*, 1994, **29**, 63.
- Giammona, G., Puglisi, G., Cavallaro, G., Spadaro, A. and Pitarresi, G., *J. Controlled Release*, 1995, **33**, 261.
- Spadaro, G., Dispensa, C., Giammona, G., Pitarresi, G. and Cavallaro, G., *Biomaterials*, 1996, **17**, 953.
- Giammona, G., Pitarresi, G., Tomarchio, V., Cavallaro, G. and Mineo, M., *J. Controlled Release*, 1996, **41**, 195.
- Giammona, G., Tomarchio, V., Pitarresi, G. and Cavallaro, G., *Polymer*, 1997, **38**, 3315.
- Giammona, G., Carlisi, B., Cavallaro, G., Donato, I., Pinio, F. and Turco Liveri, V., *Int. J. Pharm.*, 1990, **64**, 239.
- Cavallaro, G., Giammona, G., La Manna, G., Pitarresi, G. and Turco Liveri, V., *J. Therm. Anal.*, 1994, **42**, 869.
- Cavallaro, G., Giammona, G., La Manna, G., Palazzo, S., Pitarresi, G. and Turco Liveri, V., *Int. J. Pharm.*, 1993, **90**, 195.
- Giammona, G., Carlisi, B., Pitarresi, G., Cavallaro, G. and Turco Liveri, V., *J. Controlled Release*, 1992, **22**, 197.
- Turco Liveri, V., Cavallaro, G., Giammona, G., Pitarresi, G. and Turco Liveri, M. L., *Int. J. Pharm.*, 1993, **99**, 285.
- Cavallaro, G., Giammona, G., Goffredi, M., La Manna, G., Pitarresi, G. and Turco Liveri, V., *J. Biact. Comp. Polym.*, 1994, **9**, 101.
- Umehara, T., Kuwabara, S., Mashimo, S. and Yagihara, S., *Biopolymers*, 1990, **30**, 649.
- Giammona, G., Carlisi, B. and Palazzo, S., *J. Polym. Sci. Polym. Chem.*, 1987, **25**, 2813.
- Giammona, G., Carlisi, B., Palazzo, A. and Palazzo, S., *Boll. Chim. Farm.*, 1989, **128**, 62.
- Ueki, T., Hiragi, Y., Izumi, Y., Tagawa, H., Kataoka, M., Muroga, Y., Matsushita, T. and Amemiya, Y., *Photon Factory Activity Report*, **1**, V7, V29, V170, 1983.
- Guinier, A. and Fournet, G., in *Small-Angle Scattering of X-Rays*. Wiley, New York, 1955.
- Porod, G., *Acta Physica Austriaca*, 1948, **2**, 133.
- Kratky, O. and Porod, G., *J. Colloid Sci.*, 1949, **4**, 35.
- Zimm, B. H., *J. Chem. Phys.*, 1948, **16**, 1093.
- Antoni, G., Neri, P., Pedersen, T. G. and Ottesen, M., *Biopolymers*, 1974, **13**, 1721.
- Debye, P., *J. Phys. Colloid. Chem.*, 1947, **51**, 18.
- de Gennes, P. G., *Scaling Concepts in Polymer Physics*. Cornell University Press, Ithaca, NY, 1979.
- Pispisa, B. and Palleschi, A., *Macromolecules*, 1986, **19**, 904.
- Pispisa, B., Palleschi, A. and Paradossi, G., *J. Phys. Chem.*, 1987, **91**, 1546.
- Pispisa, B., Paradossi, G., Palleschi, A. and Desideri, A., *J. Phys. Chem.*, 1988, **92**, 3422.
- Chiessi, E., Palleschi, A., Paradossi, G., Venanzi, M. and Pispisa, B., *J. Chem. Res. (S)*, 1991, 248.
- Chiessi, E., Branca, M., Palleschi, A. and Pispisa, B., *Inorg. Chem.*, 1995, **34**, 2600.
- Wunderlich, H. and Mootz, D., *Acta Crystallogr. Sect. B*, 1971, **27**, 1684.
- Andersen, A. M., *Acta Chem. Scand. Ser. B*, 1975, **29**, 239.
- Nemethy, G., Pottle, M. S. and Scheraga, H. A., *J. Phys. Chem.*, 1983, **87**, 1883.
- Saudek, V. and Rypacek, F., *Int. J. Biol. Macromol.*, 1988, **10**, 277.